

Lasers in Manufacturing Conference 2019

# Simulation of the Temperature Profile on the Cutting Edge in Laser Fusion Cutting

Ulrich Halm<sup>a\*</sup>, Markus Niessen<sup>b</sup>, Dennis Arntz<sup>c</sup>, Arnold Gillner<sup>b,c</sup>, Wolfgang Schulz<sup>a,b</sup>

<sup>a</sup>Nonlinear Dynamics of Laser Processing NLD, RWTH Aachen University, Steinbachstr. 15, 52074 Aachen, Germany

<sup>b</sup>Fraunhofer Institute for Laser Technology, Steinbachstr. 15, 52074 Aachen, Germany

<sup>c</sup>Chair for Laser Technology LLT, RWTH Aachen University, Steinbachstr. 15, 52074 Aachen, Germany

---

## Abstract

Striations on the cutting edge are one of the essential quality reducing features in laser fusion cutting. Research shows that dynamics in the motion of the thin melt film on the cutting front have a strong effect on the formation of striations. A highly resolved 3D simulation of the melt film dynamics provides a detailed insight into the evolution of the temperature profile on the cutting edge. The horizontal streak analysis of the simulated temperature explains the connection between strongly changing surface temperatures and pronounced striations. The comparison with experimental results shows good correspondence with the tendency that a reduction of the dynamics of the temperature profile on the cutting edge leads to a reduced striation depth. Measures to reduce the striation depth should aim to a reduced dynamics of the surface temperature. Examples of such measures are Gaussian beam distributions or oscillation of the beam axis into lateral direction.

Keywords: Simulation, Laser Fusion Cutting, Streak Analysis

---

## 1. Introduction

High-performance laser fusion cutting is well established in industry. Modern energy-efficient fiber and disc laser systems show a larger tendency to quality reducing features like striations and adherence of dross compared to energy-intensive CO<sub>2</sub> laser systems. For dross-free cuts, the essential quality criteria are angular tolerance  $u$  and mean surface roughness  $R_z$  as defined in ISO 9013 (2017). A common setup for industrial sheet metal cutting tasks is: stainless steel, thickness  $t=6$  mm, laser power  $P_L=4.8$  kW, feed velocity  $v_0=1.4$  m/min, assist gas pressure  $p_g=10..20$  bar, focal position relative to the surface  $z_0=-8..+8$  mm. Modern fiber laser system can obtain mean surface values  $R_z \geq 40$   $\mu\text{m}$  (Arntz et al., 2018) in the lower third of the

---

\* Corresponding author. Tel.: +49-241-8906-680; fax: +49-241-8906-121.  
E-mail address: ulrich.halm@nld.rwth-aachen.de

cutting edge, while CO<sub>2</sub> laser systems can reach values below  $R_z \leq 10 \mu\text{m}$  (Librera et al, 2015). Theoretical investigations using linear stability analysis by Poprawe et al. (2010) show that the absorption characteristics of CO<sub>2</sub> laser radiation has a weaker exciting effect on existing melt waves compared to fiber and disc laser radiation. Measures to reduce excitation of melt waves like modulation (Vossen et al., 2013) or polarized laser radiation (Rodrigues et al., 2018) were tested in literature, however a drastic reduction of the mean surface roughness for fiber and disc lasers has not been demonstrated until today. To enhance the understanding of the interaction between melt film dynamics and formation of striations on the cutting edge, a 3D simulation is used. Therefore:

- Quality features are extracted from simulation results.
- Horizontal streak analysis of the surface temperature is performed at 75% sheet thickness.
- Formation of striations is tracked down from the temporal evolution of the surface temperature.

The process parameters used for process simulation are taken from Hirano and Fabro, 2011, because of better analyzability in the process simulation: stainless steel, sheet thickness  $t=3 \text{ mm}$ ,  $v_0=1.6 \text{ m/min}$ ,  $P_L=8 \text{ kW}$ . The application of the process simulation to process parameters more relevant in industry is subject of current work.

## 2. Process Simulation

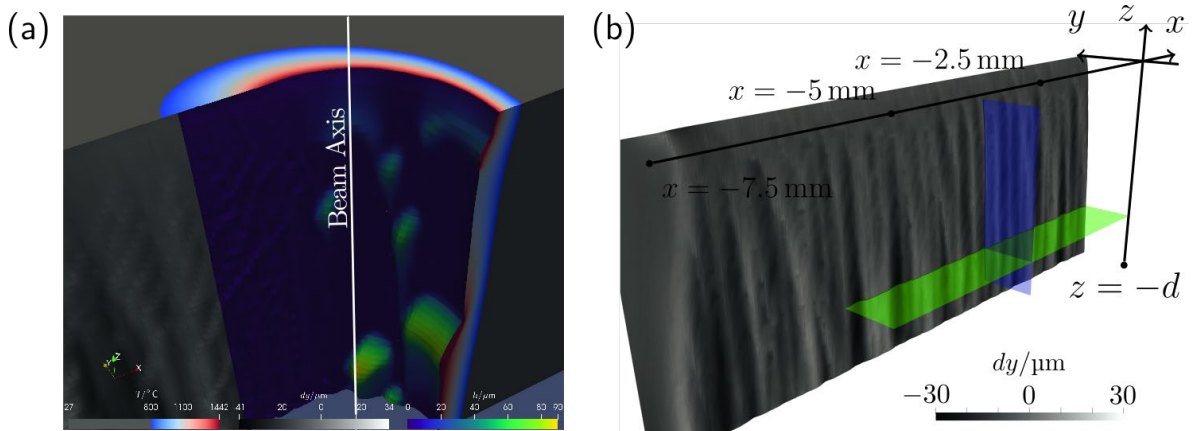


Fig. 1. (a) Visualization of sheet metal cutting from process simulation: The result is clipped in the x-z plane. The laser beam is moved to the right. The solid material is displayed in gray for temperatures below 800°C and with false-colors between blue and red for temperatures above 800°C. The melt film thickness  $h$  is indicated with false-colors between violet (no melt film) and yellow. On the left part of the image the cutting edge is visible, the deviation from the mean value in one z-layer  $dy$  is indicated in gray-scale; (b) Visualization of the cutting edge from process simulation with deviation from the mean value in one z-layer  $dy$ . The green and blue planes display the cuts to determine the quality criteria mean surface roughness  $R_z$  and angular tolerance  $u$ .

A reduced model designed for laser fusion cutting is used to carry out the simulations (Jansen et al., 2017, Halm, 2018). The 3D process simulation is based on the following assumptions:

- Melt film dynamics can be described by an integral model using a quadratic approach for axial and azimuthal velocities inside the thin melt film.
- Time scale separation of assist gas flow and melt flow allows separation of simulation of melt film dynamics and gas flow. A parametrized distribution of pressure and tension forces is used in calculation.
- Small effect of the adhesion of melt at the bottom surface of the sheet on the melt film dynamics. Thus the formation of dross is neglected in this model and an outflow condition is used in calculation.

- Temperature dependent material properties have no essential impact on the qualitative structure of the solution.
- Beam propagation is performed by ray-tracing, thus wave-optic effects are neglected.

The process simulation describes the spatial and temporal distribution of the essential solution quantities temperature, mass flux, pressure and position of the two free boundaries solid-liquid and liquid-gaseous. For analysis the measures surface roughness  $R_z$ , angular tolerance  $u$ , surface temperature  $T_s$ , absorbed heat flux density  $q_a$ , temperature gradient into solid  $q_s$  can be derived directly from simulation.

### 3. Horizontal Streak Analysis

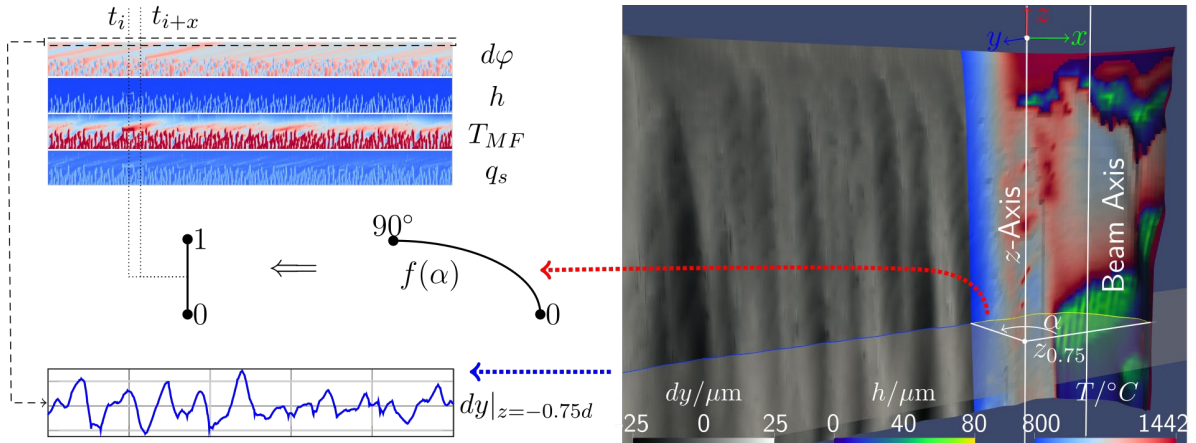


Fig. 2. Principal of horizontal streak analysis from process simulation.

On the right-hand side of figure 2 a simulation result is displayed, indicating the melt film thickness  $h$  in false-colors from dark-blue to yellow, if a melt film is present, and the melt front temperature  $T_{MF}$  in false colors between blue and red. For temperatures above the melting temperature the surface of the solid phase is overlaid by the melt film. For  $x < 0$  (behind the  $z$ -axis) the resulting cutting edge is visible and the deviation in  $y$ -direction from the mean value in one  $z$ -layer is displayed in gray-scale. At  $z = -0.75 t$  (blue line)  $dy$  reflects the roughness script which is used to determine the surface roughness value  $R_z$  at 75% depth (lower left). For the horizontal streak analysis the quantities

- radial deviation of melting front position from temporal mean value  $d\varphi$
- melt film thickness  $h$
- temperature at melting front  $T_{MF}$
- heat flux density into solid material  $q_s$

are plotted against the angle  $\alpha$ . This plot is mapped to a line of length 1 displaying the value of the quantity in false-colors between blue and red. By concatenating multiple lines for multiple time steps  $t_i$ , a horizontal streak image of the selected quantity is generated.

This streak image now indicated the temporal evolution of a quantity into  $x$ -direction and the distribution along the cutting front from the apex (bottom) to the side (top) for a selected  $z$ -layer. The topmost pixel row of the deviation  $d\varphi$  directly reflects the surface roughness script  $dy(x=x_0+v_0 t)$ . Blue parts indicate negative deviations and are related to the minimal  $y$  values inside the cutting kerf (tip of a single striation). Red parts indicate maximum positive deviations and represent the grooves between the striations. As long as no melting occurs, the deviation is (besides projection along the arc) constant in time and can be traced to its

origin inside the streak image. The location of this origin can be found at the lower left of the current position at a smaller time index and at a position  $\alpha$  closer to the melt front apex.

#### 4. Analysis

The presented method for horizontal streak analysis is applied to dynamic laser cutting simulations with the process parameters given by Hirano and Fabro (2011): sheet thickness  $d=3$  mm, laser power  $P_L=8$  kW, feed velocity  $v_0=1$  m/min, focal position  $z_0=0$  (sheet surface), rayleigh length  $z_R=30$  mm, laser spot radius  $w_0=850$   $\mu\text{m}$ , assist gas pressure  $p_g=2.5$  bar using a TruDisk10002 disc laser. The surface profile is analyzed at 75% sheet thickness  $z=0.75$  t and the deviation from the mean value  $dy$  is plotted over a distance of  $x=5$  mm.

##### 1.1. Trace of Striations

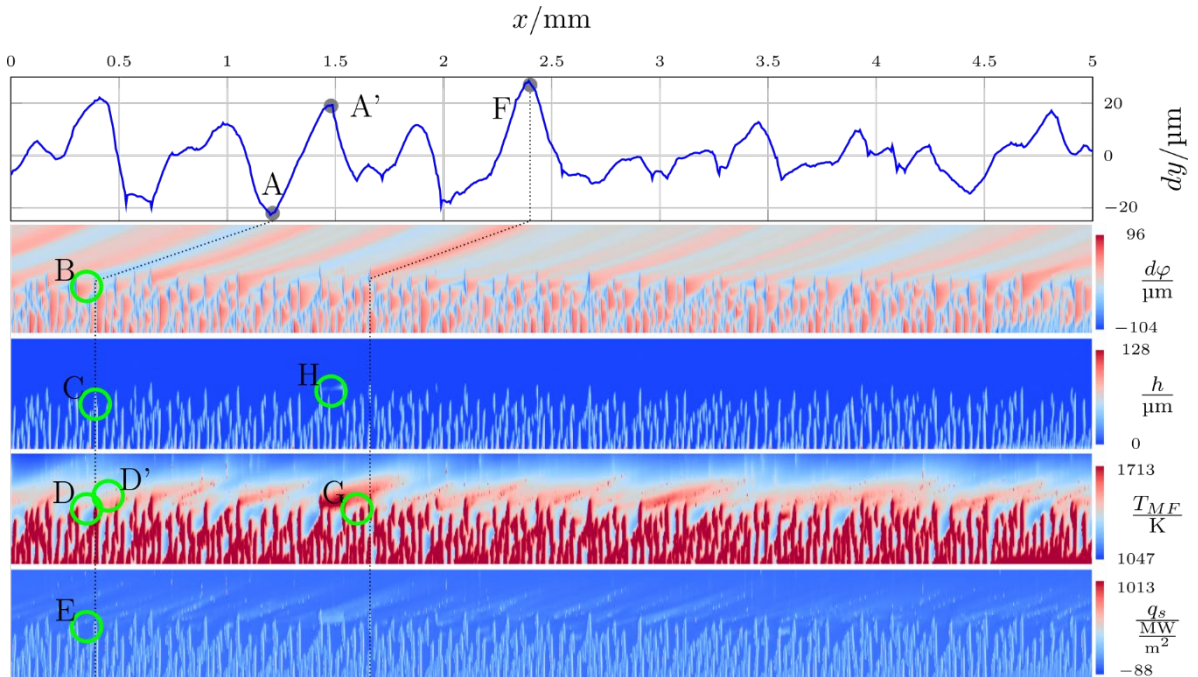


Fig. 3. Surface profile of cutting edge  $dy(x)$  at 75% sheet thickness and horizontal streak images of deviation of melt front  $d\varphi$ , melt film thickness  $h$ , melt front temperature  $T_{MF}$  and heat flux density into solid  $q_s$ .

To track down the origin of individual striations, the minimum and maximum deflections of the profile are aligned to the horizontal streak images of the quantities radial deviation  $d\varphi$ , melt film thickness  $h$ , surface temperature of the solid phase  $T_{MF}$  and heat flux density into solid material  $q_s$ . The topmost pixel row of each quantity describes the temporal evolution at the transition point from the cutting front to the cutting edge, the lowermost the temporal evolution at the apex of the cutting front. Figure 3 shows these plots for a feed velocity of  $v_0=1$  m/min. A minimum deviation at (A) followed by a maximum deviation at (A') correspond to a particular striation. By following the deviation  $d\varphi$  inside the streak image from the position on the side (A) to its origin (B), the origin of this striation can be found at a position of around  $45^\circ$  on the cutting front. The evolution of the melt film thickness  $h$  at (C) indicates, that one individual melt wave is responsible for the

significantly larger deflection of the melting front. The preliminary surface temperature  $T_{MF}$  (D) is significantly smaller than after crossing of the melt wave (D'). The heat flux density into the material  $q_s$ , which can be understood as the energy content, is significantly smaller (E) before the melt wave traveled across this position. This means: the melt wave (C) deposited material on the cutting front due to small energy content and small temperature of the solid material, causing a large ripple tip (A). The melt wave itself deposited energy inside the solid material and increased the surface temperature, so that the next melt wave created a significant groove (A'), which together with (A) created a pronounced striation.

This mechanism is also responsible for the largest groove visible in the surface roughness plot (F), whose origin is found in a larger surface temperature than the average surface temperature in advance of the melt wave (G). This larger surface temperature was caused by two melt waves with a very small distance (H), which heated up the front in advance of the melt wave causing the groove (F).

## 1.2. Variation of Feed Velocity

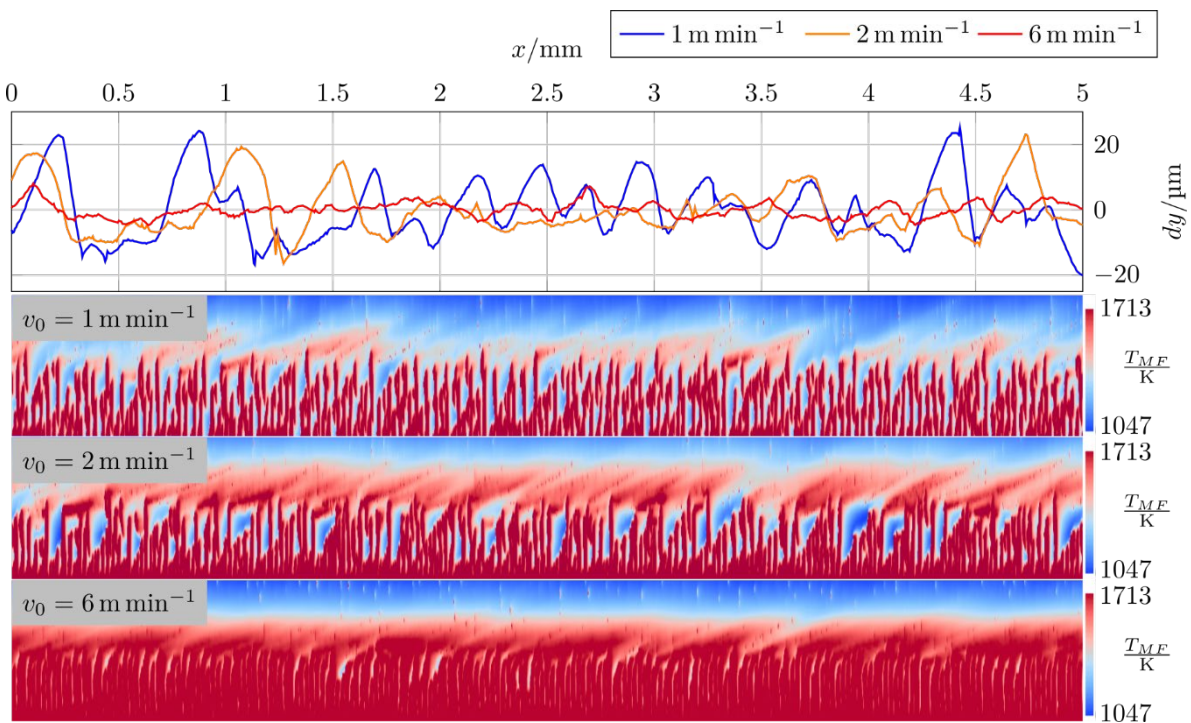


Fig. 4. Surface profile of cutting edge  $dy(x)$  at 75% sheet thickness and horizontal streak images of melt front temperature  $T_{MF}$  for different feed velocities  $v_0$ .

To analyze the effect of a homogenization of the surface temperature  $T_{MF}$ , the feed velocity is increased to  $v_0=2$  m/min and  $v_0=6$  m/min. Hirano and Fabro (2011) demonstrated that an increased feed velocity leads to a drastically reduced mean surface roughness. Figure 4 indicates that the dynamic simulation calculates considerably smoother surface profiles for larger feed velocities. The horizontal streak images of the surface temperature at larger feed velocities show a clearly more homogeneous distribution compared  $v_0=1$  m/min. The corresponding mean surface roughness values of  $R_{z,1mpm}=33$   $\mu\text{m}$ ,  $R_{z,2mpm}=26$   $\mu\text{m}$  and  $R_{z,6mpm}=9$   $\mu\text{m}$

underestimate the experimental values by a factor of 2. However the tendency is correctly reproduced. The deviance between simulation and experiment might be caused by additional effects not considered in the simulation so far like surface tension and temperature dependent material properties or fluctuations in the intensity of the laser light, the assist gas flow and the material itself.

## 5. Conclusion and Outlook

A 3D simulation of the melt film dynamics in laser fusion cutting has been used to analyze the temporal evolution of the simulated quantities deviation of the melt front position, melt film thickness, surface temperature of the solid phase and heat flux density into the solid phase. Using the horizontal streak analysis, the origin of particular striations has been tracked down. Non-homogeneous surface temperature distributions were identified as origin of irregularities in the surface profile plot and thus to pronounced striations. A homogenization of the surface temperature by an increase of the surface temperature lead to a drastically reduced mean surface roughness.

Other means to homogenize the surface temperature on the side of the cutting front should be analyzed. This includes: beam shapes with a smoother slope on the side like combined Gaussian and top-hat beams or spatial and temporal modulation of the beam.

## Acknowledgements

The presented investigations were carried out at RWTH Aachen University within the framework of the Collaborative Research Centre SFB1120-236616214 "Bauteilpräzision durch Beherrschung von Schmelze und Erstarrung in Produktionsprozessen" and funded by the Deutsche Forschungsgemeinschaft e.V. (DFG, German Research Foundation). The sponsorship and support is gratefully acknowledged.

## References

- Arntz, D., Petring, D., Stoyanov, S., Jansen, U., Schneider, F., Poprawe, R., 2018. In situ visualization of multiple reflections on the cut flank during laser cutting with 1  $\mu\text{m}$  wavelength, in *Journal of Laser Applications* 30, 032206 (2018); DOI: 10.2351/1.5040614.
- Librera, E., Riva, G., Safarzadeh, H., und Previtali, B., 2015. On the use of areal roughness parameters to assess surface quality in laser cutting of stainless steel with CO<sub>2</sub> and fiber sources, *Procedia CIRP*, 33:532 – 537. 9th CIRP Conference on Intelligent Computation in Manufacturing Engineering - CIRP ICME '14.
- Halm, U., 2018. Simulation hochdynamischer Vorgänge in der Schmelze beim Laserstrahlschneiden, Dissertation Verlag Dr. Hut, ISBN: 978-3-8439-3884-6
- Hirano, K., Fabbro, R., 2011. Experimental investigation of hydrodynamics of melt layer during laser cutting of steel. *Journal of Physics D: Applied Physics*, 44(10):105502.
- ISO 9013:2017(E), 2017. Thermal cutting – Classification of thermal cuts – Geometrical product specification and quality tolerances. Standard, International Organization for Standardization, Geneva, CH.
- Jansen, U., Niessen, M., Hermanns, T., Arntz, D., Poprawe, R., Schulz, W., 2017. Boundary Layer Approximation for Melt Film Dynamics in Laser Fusion Cutting. In: 22nd International Congress on Modelling and Simulation, MODSIM 2017, Hobart, Australia.
- Poprawe, R., Schulz, W., und Schmitt, R., 2010. Hydrodynamics of material removal by melt expulsion: Perspectives of laser cutting and drilling. *Physics Procedia*, 5:1 – 18. *Laser Assisted Net Shape Engineering 6*, Proceedings of the LANE 2010, Part 1.
- Rodrigues, G. C., Vorkov, V., und Duflou, J. R., 2018. Optimal laser beam configurations for laser cutting of metal sheets. *Procedia CIRP*, 74:714 – 718. 10th CIRP Conference on Photonic Technologies, LANE 2018.
- Vossen, G., Hermanns, T., und Schüttler, J., 2013. Analysis and optimal control for free melt flow boundaries in laser cutting with distributed radiation. *ZAMM – Journal of Applied Mathematics and Mechanics / Zeitschrift für Angewandte Mathematik und Mechanik*, 95(3):297–316.